

Influence of laser irradiation on the optical properties of $\text{As}_{40}\text{Se}_{45}\text{Sb}_{15}$ thin films by thermal evaporation technique

Ramakanta Naik*

Physics Department, Utkal University, Bhubaneswar, Odisha, India

*Corresponding author. Tel: (+91) 6742567079; E-mail: ramakanta.naik@gmail.com

Received: 26 November 2014, Revised: 15 March 2015 and Accepted: 18 March 2015

ABSTRACT

The present paper highlights the optical properties change in thermally evaporated $\text{As}_{40}\text{Sb}_{15}\text{Se}_{45}$ amorphous film of 800 nm thickness with laser irradiation. The as-prepared and illuminated films were studied by X-ray diffraction, Energy dispersive X-ray analysis. The optical properties were calculated from the transmission spectra obtained from Fourier Transform Infrared Spectroscopy. The band gap is decreased by 0.22 eV due to photo induced effects causing photo darkening. The refractive index is found to be increased due to increase in structural disordering. These optical properties changes are due to the change of homopolar bond densities which can be seen from the core level peak shifting in XPS spectra. The optical constants such as refractive index, band gap of the material plays a major role in the preparation of the device for a particular wavelength. Selecting suitable pairs of chalcogenide glasses with different optical gaps, one can modify the parameters of the light sensitive layers and use them for optical recording. Copyright © 2015 VBRI Press.

Keywords: CdS; Mn; phase transition; blue shift; cole-cole plots.



Ramakanta Naik is DST-INSPIRE faculty in the Department of Physics, Utkal University, Bhubaneswar, India. He has received his PhD degree in Physics from Indian Institute of Science, Bangalore in 2010. His major research interest is on amorphous semiconducting chalcogenide materials and their optical properties study. He is deeply involved in photo induced optical change in chalcogenide thin films. He is working on the thin film preparation of these materials by thermal evaporation technique and the application on optical devices.

Introduction

The semiconductor is an essential material in electronic device fabrication such as diodes, laser diodes (LD), light emission diodes (LED), sensors, solar cells, thermoelectric devices, etc. [1-3]. The band-gap energy is a very important property of the semiconductor and depends greatly on the material. The optical band gap of the material plays a major role in the preparation of the device for a particular wavelength. The band-gap energy value is modified by photo induced effects which is prominently observed in chalcogenide semiconductors based on S, Se, and Te. They have many unique optical properties, which can be used for a wide variety of application like solar cells, antireflection coating, optical limiting, and manufacture of filters, infrared power delivery, IR emitter, optical rewritable data, IR detector, gratings and optical recording media [4-8].

Chalcogenide based films are used for low power consumption phase change memory applications [9].

The photo induced effects are prominently visible in the class of amorphous chalcogenide materials due to the flexible structure which are instantaneously affected by the external stimuli like heat, laser light, e-beam, pressure, etc. The lone-pair character of the valence tails lead to very rich behavior under the influence of light. These create different metastable states and related changes of the optical, electrical parameters. Such changes could be reversible or non-reversible, directed from crystalline to amorphous state or from amorphous to crystalline one, depending on the composition, structure, technology or type of excitation [10]. This processes offer the possibility of using amorphous chalcogenide semiconductors for high-density information storage, high-resolution display devices and fabrication of diffractive optical elements, direct structure fabrication by electron lithography and single-stage information recording [11,12].

Furthermore, the broad range of photo-induced effects that the chalcogenide glasses exhibit, often accompanied by large changes in the optical constants [13,14] and, particularly, shifts in the absorption edge (i.e., photo darkening or photo bleaching). Photo induced changes of optical transmittivity and reflectivity, index of refraction, changes of reactivity, rates of diffusion and inter-diffusion, viscosity and the state (phase) have been observed in many

materials. The optical properties like extinction coefficient (k), absorption coefficient (α), optical band gap (E_g) and Urbach's energy E_u are important parameters and can be utilized from absorption spectra, transmission spectra and reflection spectra. Large number of research groups throughout the world are trying to change the material properties (optical, structural, electrical etc.) for enhancing the device performance by using different techniques such as different deposition techniques, irradiation techniques (laser irradiation, swift heavy ion irradiation, gamma-ray irradiation etc), doping techniques etc. All investigated changes in optical parameters are irreversible, due to which these type of materials can be used for archival memory, for creation of optical, integrated optical elements, which need high local changes of optical parameters. Selecting suitable pairs of chalcogenide glasses with different optical gaps, one can modify the parameters of the light sensitive layers and use them for optical recording.

In the present study, the effect of laser irradiation on the optical, properties of $As_{40}Se_{45}Sb_{15}$ thin film is presented. The study of the optical absorption spectra in chalcogenide glasses provides essential information about the band structure and the energy band gap. The optical band gap of the material plays a major role in the preparation of the device for a particular wavelength, which can be modified by the addition of impurity [14]. So, the influence of metallic additives on the optical properties has been an important issue in the case of chalcogenide glasses. The ternary Sb-As-Se glasses are formed by adding Sb atoms in the As-Se system. The corresponding substitution does not alter drastically the basic structure of glass, since both As and Sb are isovalent elements. But, the Se amount is reduced by substitution of Sb. Optical analysis of the present case was carried out by FTIR spectrometer and it was found that the optical band gap of the film was decreased due to laser light irradiation and the other optical parameters changes accordingly. X-ray Photoelectron spectra (XPS) analysis gives information about the changes in bonding in the films. XRD pattern of both as-prepared and light irradiated thin films of $As_{40}Se_{45}Sb_{15}$ shows the amorphous nature. The optical constant which is changed due to laser illumination has not been studied for this type of material. These new findings can be used for fabrication of holographic recording materials, photo lithography etc.

Experimental

Materials

High purity As (99.999 % pure), Sb (99.999 % pure), and Se (99.999 % pure) were purchased from Sigma-Aldrich Chemical Co. and used as received. Bulk glass of $As_{40}Se_{45}Sb_{15}$ was prepared by melt quenching technique. Materials of (99.995% pure) As, Se and Sb were weighed according to their atomic percentage and after that sealed in a quartz ampoule in a vacuum of $\sim 10^{-5}$ Torr. The sealed ampoule was kept inside a rotating furnace at 1000 °C for 36 h to make the melt homogeneous. The bulk glass was obtained by quenching the ampoule in ice cooled water. Thin films were prepared by thermal evaporation method at a base pressure of 1×10^{-5} Torr from the prepared bulk glass onto the glass substrates (microscope slides). During the

deposition process (at normal incidence), the substrates were suitably rotated in order to obtain the films of uniform thickness. The thicknesses of the films were around 800 nm.

Methods

The amorphous state of the film was checked by X-ray (Philips type 1710 with Cu as target and Ni as filter, $\lambda=1.5418 \text{ \AA}$) Diffractometer (XRD). The elemental composition of the as-prepared film was checked by energy dispersive X-ray analysis (EDAX) in Sirion XL 40 in which EDAX is attached. The scan was done at 20 kV with 40 μA emission current exposing a sample of 1 cm^2 size at 2×10^{-7} Torr pressure. The estimated average precision was less than 3 % in atomic fraction in each element (Table 1). To study the photo induced changes, we irradiated the film at room temperature by a diode pumped solid state laser (DPSS) of wavelength 532 nm with a power of 40 mW. The film was mounted on a sample holder and the laser light was focused into 2 mm wide spot. The optical transmission spectra of the as-prepared and irradiated films were taken by the Fourier Transform Infrared (FTIR) spectrometer (Bruker Optics (IFS66v/S) in the visible wavelength range 600-1200 nm. We have used XPS to analyze the new bonds formed due to photo induced effect. It is a useful surface analytical technique to study the chemical state and local environment of an atom. The XPS core level spectra were obtained with monochromatic $Mg K_{\alpha}$ X-rays (1253.6 eV) at a vacuum of 10^{-9} Torr in Multilab 2000 Thermo Scientific UK instrument. The XPS data consisted of survey scans over the entire binding energy (BE) and selected scans over the core level peaks of interest. An energy increment of 1 eV was used for recording the survey spectra and 0.05 eV for the case of core level spectra. The core level peaks were recorded by sweeping the retarding field and using the constant pass energy of 30 eV. The data were averaged over three scans. The reproducibility of the measurements was checked on different regions of the investigated surfaces. For insulators such as glasses, the charging effect can change the BE of the electrons from sample to sample. Hence, the measurement of the absolute BE of electrons from a specified energy level is not reliable. The C 1s line from either adventitious carbon or intentionally added graphite powder on the surface has been widely used for charge referencing. For this study, the adventitious carbon was used as a reference and the BE of the reference C 1s line was set as 284.6 eV. For each sample, a calibration factor was calculated from the difference between the measured C 1s BE and the reference value 284.6 eV [15]. The original BE data were corrected according to the calibration factor. All the measurements were performed at room temperature (300 K).

Results and discussion

Fig. 1 shows the XRD patterns of the as-prepared and irradiated $As_{40}Se_{45}Sb_{15}$ film. The absence of sharp structural peaks for both the films confirms the amorphous nature of the samples. The width of 2θ was from 23° - 38° . The diffractograms are very similar to the point that no

differences can be recorded between the two films. The EDAX analysis carried out on the as-prepared film suggest that their compositions are very close to the starting materials (Table 1). Fig. 2 shows the presence of Se, Sb and as in the as-deposited film with nearly equal chemical composition.

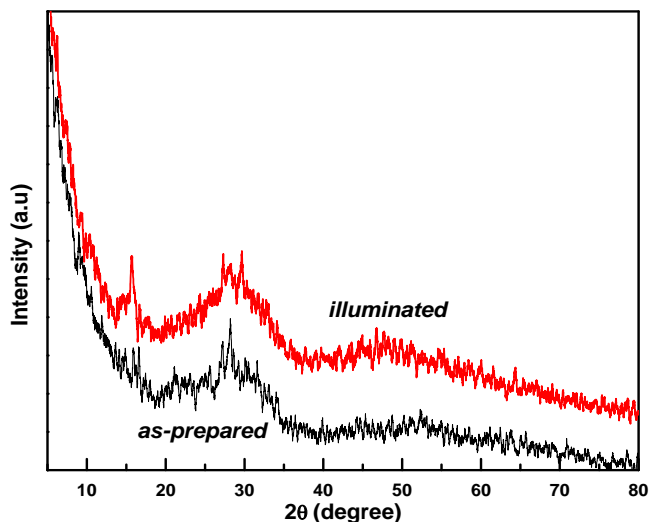


Fig. 1. XRD pattern of as-prepared and irradiated $As_{40}Se_{45}Sb_{15}$ thin film.

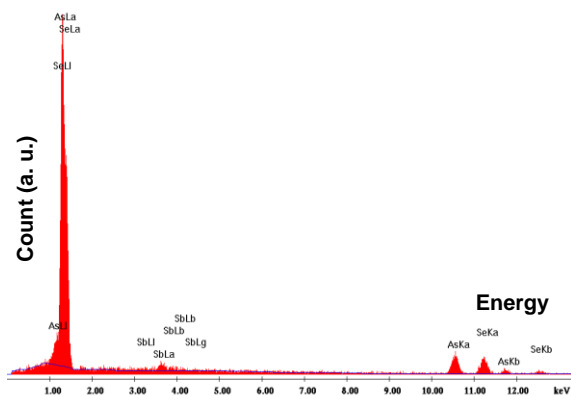


Fig. 2. EDAX spectrum of the $As_{40}Se_{45}Sb_{15}$ thin film.

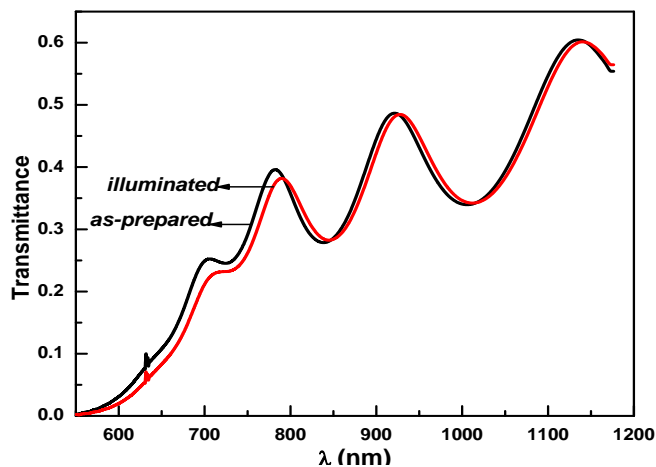


Fig. 3. Transmission spectra of as-prepared and irradiated $As_{40}Se_{45}Sb_{15}$ thin film.

The transmittance spectra of both the films are plotted in Fig. 3 which shows the ‘non-shrinking’ interference fringes at higher wavelength (600–1200nm) that indicates the homogeneity and smoothness of the deposited films. The optical constants were calculated by using Swanepoel Envelope method [16].

Table 1. The measured elemental composition from EDAX for $As_{40}Se_{45}Sb_{15}$ thin film.

Element	Wt%		At%	
	Observed	Calculated	Observed	Calculated
As	35.27	35.77	39.65	40
Sb	20.98	21.82	15.12	15
Se	43.75	42.41	45.23	45

The refractive index for the as-prepared and irradiated films is shown in Fig. 4. The refractive index n can be fitted to the Cauchy dispersion relationship [17]

$$n = \left(a + \frac{b}{\lambda^2} \right) \quad (1)$$

This can be used for extrapolation of the values of the refractive index to shorter wavelength region as shown in Fig. 4.

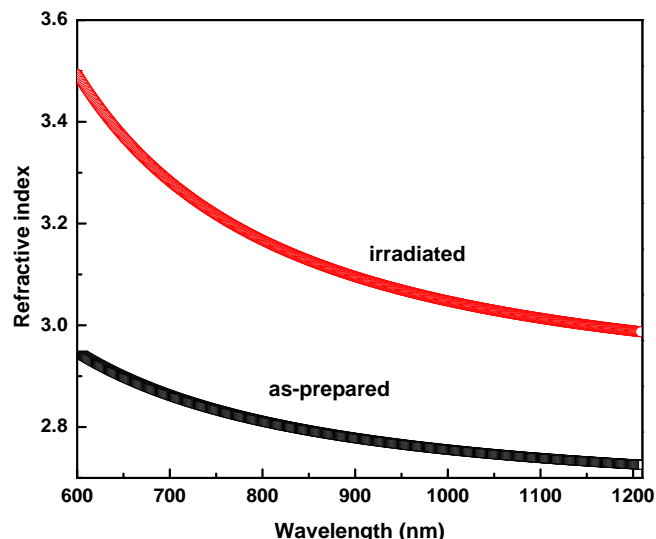


Fig. 4. n vs λ for the $As_{40}Se_{45}Sb_{15}$ thin films.

The decrease in the value of the refractive index with wavelength shows the normal dispersion behavior of the material. It was also observed that the value of refractive index increased with light exposure, which was supported by previous studies on various other types of high intensity photo exposure [18, 19]. This is an indication of photo refraction (optical densification) caused by light exposure. Increase in refractive index upon light exposure is a consequence of local structural modification, which brings the local structure of the film close to bulk glass. The absorption coefficient (α) has been calculated by using the equation

$$\alpha = \frac{1}{d} \ln\left(\frac{1}{T}\right) \quad (2)$$

where T is the transmission and d is the thickness of the film. The variation of absorption coefficient with $h\nu$ is shown in **Fig. 5**. Whenever any electromagnetic wave propagates inside the medium, its loss by absorption or scattering process is represented by absorption coefficient. It is clear from this plot that α decreases with wavelength and increases upon light exposure [20, 21]. It has been observed that the absorption coefficient increases with laser irradiation. In crystalline materials, the fundamental edge is directly related to transitions from the conduction and valence band, and associated with direct and indirect band gaps, whereas in the case of amorphous material the transitions are termed non-direct owing to the absence of an electronic band structure in k -space. In the absorption process, a photon of known energy excites an electron from a lower to a higher energy state, corresponding to an absorption edge.

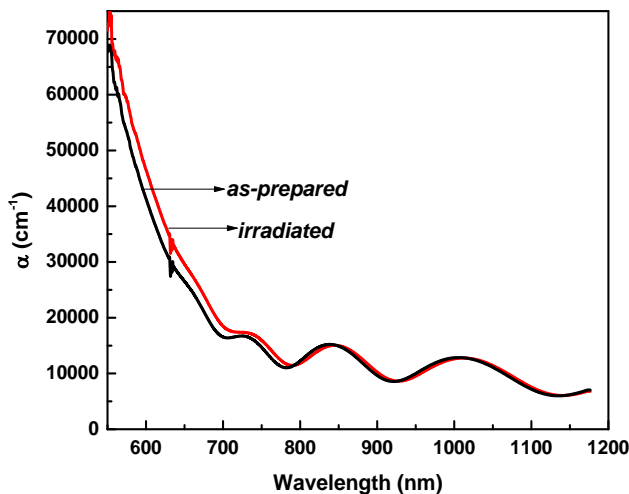


Fig. 5. α vs λ for the as-prepared and irradiated $\text{As}_{40}\text{Se}_{45}\text{Sb}_{15}$ thin film.

The optical absorption spectrum is the most productive tool for developing the energy band diagram. The absorption coefficient of amorphous semiconductors in the high absorption region ($\alpha \geq 10^4 \text{ cm}^{-1}$) follows an exponential law according to Tauc [22].

$$\alpha h\nu = B(h\nu - E_g)^m \quad (3)$$

where B is the constant (Tauc parameter), E_g is the optical energy gap of the material and m determines the type of transition ($m=1/2$ for direct allowed transition and $m=2$ for indirect allowed transition) [22, 23]. The best fit of the experimental results of as-prepared and irradiated thin films of $\text{As}_{40}\text{Se}_{45}\text{Sb}_{15}$ using Eq. (3), with $m = 2$ i.e., the variation curve of $(\alpha h\nu)^{1/2}$ with photon energy ($h\nu$) (shown in **Fig. 6**) is found to be identical to that of the elemental amorphous semiconductor. This indicates that the absorption in as-prepared and irradiated thin films of $\text{As}_{40}\text{Se}_{45}\text{Sb}_{15}$ is due to non-direct transition. Plotting the

dependence of $(\alpha h\nu)^{1/2}$ on photon energy ($h\nu$) will give a straight line and the y intercept gives the value of the optical band gap (**Fig. 6**).

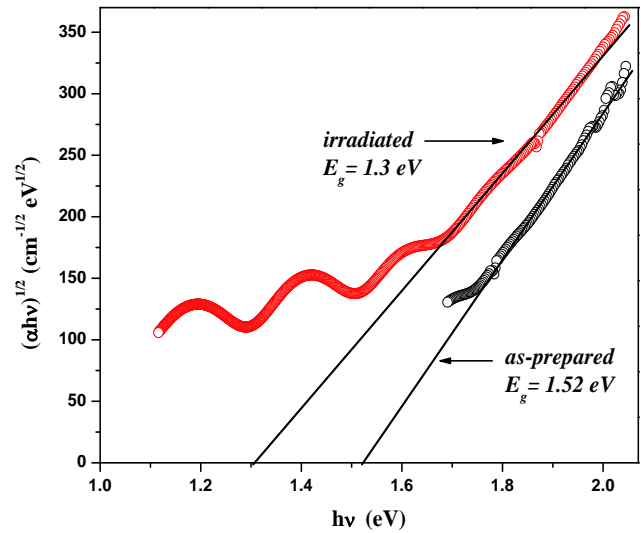
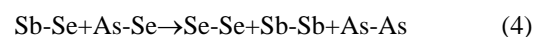


Fig. 6. $(\alpha h\nu)^{1/2}$ vs $(h\nu)$ plots for the $\text{As}_{40}\text{Se}_{45}\text{Sb}_{15}$ thin films.

The optical band gaps of the as-prepared and the illuminated films are found to be 1.52 eV and 1.30 eV respectively. The band gap of illuminated film is found to be decreased by 0.22 eV from the as-prepared film which shows photo darkening mechanism in the film. Since, the optical absorption depends on the short-range order in the amorphous states and defects associated with it, the decrease in optical band gap may be explained on the basis of “density of state model” proposed by Mott and Davis [24]. According to this model, the width of the localized states near the mobility edges depends on the degree of disorder and defects present in the amorphous structure. In particular, it is known that unsaturated bonds together with some saturated bonds are produced as the result of an insufficient number of atoms deposited in the amorphous film.

The unsaturated bonds are responsible for the formation of some of the defects in the films, producing localized states in the amorphous solids. The presence of high concentration of localized states in the band structure is responsible for the decrease of optical band gap in case of amorphous films. This decrease in the band gap may also be due to the shift in Fermi level, whose position is determined by the distribution of electrons over the localized states [25]. The decrease in optical band gap (E_g) with laser irradiation can be attributed to the reduction in the density of tail states adjacent to the band edge. Therefore, the intrinsic structural change in photo darkening process has been proposed as the increase in the Se-Se, Sb-Sb and As-As bond density and its subsequent decrease in the structural ordering.

The intrinsic structural changes are ascribed to the following photoreaction



The illumination process creates local structural disordering in $\text{As}_{40}\text{Se}_{45}\text{Sb}_{15}$ thin films with heteropolar bonds Se-Sb, As-Se being converted into Se-Se, Sb-Sb and As-As homopolar bonds.

According to Fritzsche [26], the decrease in the optical gap in the chalcogenide glasses due to photo-induced phenomena results mainly from the interaction between lone-pairs and incident photon. It is known that the lone-pair electrons occupy the top of the valence band. Therefore, the irradiation will excite the lone pair electrons just above the band-gap energy and subsequent capture on localized states somewhere close to the top of valence band (charged defects) [27]. This will lead to an upward shift of the top of the valence band, thus narrowing the band gap. Generally speaking, a decrease in the band gap (red shift in the absorption edge) is accompanied by increase in the refractive index according to Moss's rule ($E_g n^4 \sim \text{constant}$) [28]. During light irradiation, one of the Se lone pair electrons from the valence band gets excited into the conduction band, leaving behind the other in the lone pair orbital. The distance between such excited atoms is close to the covalent bond length and the spins have opposite directions. So, additional covalent bonds can be dynamically formed between excited atoms, making some of the selenium atoms threefold coordinated. The formation of the dynamical bonds causes the displacement of nearest neighbor atoms which slip away from equilibrium position, resulting in an increase in the total lone pair-lone pair interactions. It leads to the widening of the valence band, resulting in the reduction in band gap (Photo darkening) [29]. The optical parameters obtained from the fittings are given in **Table 2** which shows the changes due to photo darkening process. It shows the variation in optical band gap, τ_{auc} parameter and Urbach energy for the as-prepared and illuminated film.

Table 2. Optical parameters calculated for the as-prepared and irradiated thin film.

sample	Band gap E_g (eV)	τ_{auc} parameter ($\text{cm}^{-1/2} \text{eV}^{-1/2}$)	Urbach energy (meV)
As-prepared	1.52 ± 0.001	510 ± 4	198 ± 1
irradiated	$1.3 \pm 4 \pm 0.002$	468 ± 3	231 ± 2

The slope of the equation 3 gives the value of constant $B^{1/2}$ which includes the information on the convolution of the valence band and conduction band states and on the matrix element of optical transitions, which reflects not only the k selection rule but also the disorder induced spatial correlation of optical transitions between the valence band and conduction band [22]. Moreover, B is highly dependent on the character of the bonding. The $B^{1/2}$ for illuminated film ($468 \pm 3 \text{ cm}^{-1/2} \text{eV}^{-1/2}$) is less than the as-prepared film ($510 \pm 4 \text{ cm}^{-1/2} \text{eV}^{-1/2}$) which indicates the presence of more no of homopolar bonds due to chemical orderings in the film. The illuminated film is more disordered (chemically) than the as-prepared film, i.e., the creation of homopolar bonds after photo induced process which is confirmed from the XPS analysis discussed in the present report.

Chalcogenide glasses have been found to exhibit highly reproducible optical edges, which are relatively insensitive to preparation conditions and only the observable absorption with a gap under equilibrium conditions account for this process. In amorphous materials, a different type of optical absorption edge is observed and absorption coefficient increases exponentially with the photon energy near the energy gap. This optical absorption edge is known as the Urbach edge which also gives information regarding the degree of disorderness according to the Urbach equation [30]

$$\alpha(h\nu) = \alpha_0 \exp\left(\frac{h\nu}{E_e}\right) \quad (5)$$

where α_0 is a constant (absorption coefficient at optical band gap) and E_e corresponds to the Urbach energy (the width of the band tail of the localized states in the band gap). The above equation describes absorption of the amorphous materials in frequency range where $10^0 < \alpha < 10^4 \text{ cm}^{-1}$ [31]. In this region, transition between (defect) states in the gap and the bands take place. Plotting the dependence of $\log(\alpha/\alpha_0)$ on photon energy ($h\nu$) will give a straight line. The inverse of the slope of the straight line gives value of E_e . This gives the width of the tails of the localized states into the gap at band edges. Urbach energy E_e has been considered as a useful parameter to evaluate the degree of structural disorder [32]. The value of E_e for as-prepared and illuminated $\text{As}_{40}\text{Se}_{45}\text{Sb}_{15}$ film is 198 meV and 231 meV respectively. The higher values of Urbach energy E_e of the illuminated film over the as-prepared film clearly indicate that the illuminated film is more structurally disordered than the as-prepared film, which may be due to the creation of homopolar bonds after photo induced process.

The $\text{As}_{40}\text{Se}_{55}\text{Sb}_5$ film was irradiated for 1.5 h by DPSS laser of 532 nm wavelength and the film was kept in dark condition at room temperature up to the time of measuring XPS data. A typical XPS spectrum of $\text{As}_{40}\text{Se}_{45}\text{Sb}_{15}$ film contains many photoelectrons and Auger peaks of As, Se and Sb. But, we have considered only the core peaks such as As3d, Sb4d and Se3d for the present study. For detailed analysis, the spectra were deconvoluted into its sub peaks by the XPS data analysis software developed by Kwok called as XPSPEAK1. The Shirley baseline was used for background correction and the deconvoluted peaks were assumed to have Voigt line shapes. The Se 3d peak position for as-prepared and illuminated films is at 53.82 eV and 54.62 eV respectively as shown in **Fig. 7**. Due to spin orbit splitting, Se 3d consists of doublets corresponding to Se $3d_{5/2}$ and Se $3d_{3/2}$ (intensity ratio 5:3) with a separation of 0.8 eV which we observed from the deconvoluted peaks of the as-prepared and irradiated film. The positions of sub peaks are mentioned in the **Fig. 7**. The Se $3d_{3/2}$ peak for the irradiated film (54.94 eV) is shifted by 0.32 eV from the as-prepared (54.62 eV) one. Similarly, the shift between the as-prepared (53.82 eV) and irradiated (54.16eV) Se $3d_{5/2}$ peak is around 0.34 eV. This shifting of BE towards higher energy side is due to photo induced changes that leads to the formation of more no of Se-Se bonds rather than the

heteropolar bonds. The increase in refractive index observed for irradiated film may be attributed to the excess of Se-Se bonds [33]. This excess homopolar bonds in the irradiated film can change the local microstructure as well as grain morphology, which leads to increase in film packing density, thus increasing refractive index [20]. The As-Sb-Se film structure can be attributed as being made up of completely cross linked structure of Sb_2Se_3 and As_2Se_3 . The irradiation process causes some of the heteropolar bond transformation to homopolar bonds like equation 4 [34].

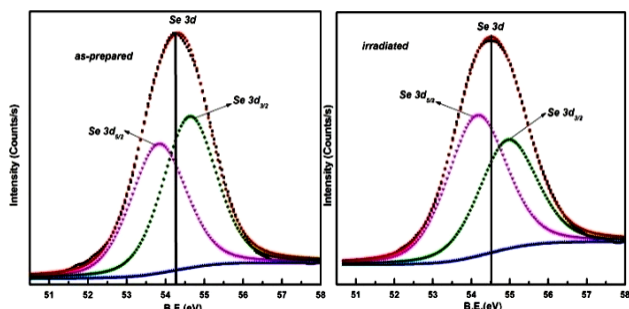


Fig. 7. Deconvoluted XPS core level spectra of Se 3d.

The peak positions of Sb 4d core level spectra for as-prepared and illuminated films are at 34.44 eV and 33.72 eV respectively (Fig. 8). The deconvoluted peaks of Sb 4d core levels are shown in fig 8. The Sb 4d_{5/2} and Sb 4d_{3/2} peaks are situated at BE of 33.75 and 35.09 eV with a gap of 1.34 eV. The photo induced process lowered the BE of both the peaks to 33.10 and 34.39 eV respectively. This peak is shifting towards the lower BE due to the formation of more Sb-Sb homopolar bonds as the electro negativity of Sb is much less than that of Se (2.55). Thus, the formation of more number of homopolar bonds by equation 6 reduces the mobility edge inside the band gap region and decreases the optical band gap.

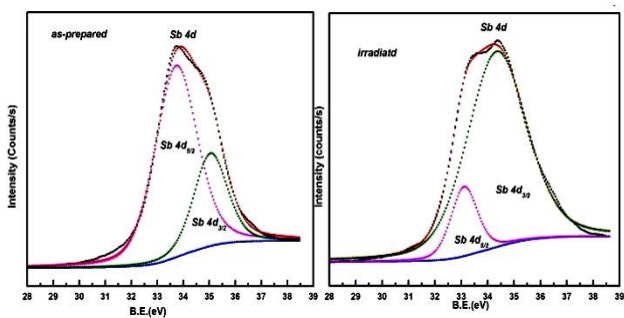


Fig. 8. Deconvoluted XPS core level spectra of Sb 4d.

The As 3d peak position for as-prepared and illuminated films are at 42.85 and 42.67 eVs respectively (Fig. 9). Due to spin orbit splitting, As 3d consists of doublets corresponding to As 3d_{5/2} and As 3d_{3/2} (intensity ratio 5:3) with a separation of 0.7 eV which we observed from the deconvoluted peaks (1-1' and 2-2'). Here, 2 and 2' denotes As 3d_{5/2} states and 1 and 1' denote As 3d_{3/2}. The two sub peaks (1-1') at 44.38 eV and 45.08 eV in the deconvoluted As 3d peak are assigned as As atoms within

$\text{AsSe}_{3/2}$ pyramidal units at higher BE. The sub peaks (2-2') at 42.28 eV and 42.98 eV are assigned as As atoms within units containing As-As homopolar bonds at lower BE [35,36]. Because, As (2.18) has a smaller electro negativity than Se (2.55), homopolar As-As bond containing units contribute the lower BE peak [33]. From the spectra of As 3d peak, it is found that due to illumination, the peak is shifting towards the lower BE due to the formation of As-As homopolar bonds. The sub peaks (3, 3') at 44.18 eV and 44.88 eV are assigned as As atoms within $\text{AsSe}_{3/2}$ pyramidal units and sub peaks (4-4') at 42.08 eV and 42.78 eV are assigned as As atoms within units containing As-As homopolar bonds at lower BE. These sub peaks show the shifting in accordance with the change.

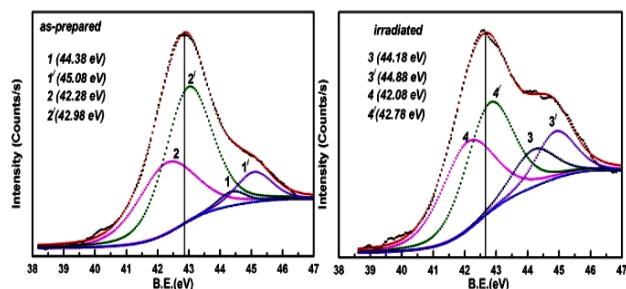


Fig. 9. Deconvoluted XPS core level spectra of As 3d.

Conclusion

In conclusion, we have investigated the photo induced microstructural transformation in thermally-evaporated amorphous $\text{As}_{40}\text{Se}_{45}\text{Sb}_{15}$ thin films when exposed to illumination. Photo induced process has changed the optical transmissivity, optical band gap, $B^{1/2}$, refractive index, extinction coefficient, etc. of the films. The laser irradiated film shows higher refractive index and lower optical band gap as compared to that of as-prepared film. The increase in refractive index is because of micro structural disorderness and is attributed to the excess homopolar bonds. The absorption mechanism in the film is due to indirect allowed transition. The decrease in optical band gap (photo darkening) is due to the change in localized states near to the band edges. The binding energy shift of different core level spectra shows the formation of more homopolar bonds which supports the decrease in optical band gap. As the optical changes occurred due to laser irradiation are irreversible, so the material can be a useful candidate for archival memory and creation of integrated optical elements, which need high local changes of optical parameters. Selecting suitable pairs of chalcogenide glasses with different optical gaps, one can modify the parameters of the light sensitive layers and use them for optical recording.

Acknowledgements

The authors thank Department of Science and Technology (DST), Govt of India for DST-INSPIRE Research grant and using the National Facility for Optical Spectrometry at Department of Physics and Surface Science facility, Indian Institute of Science (IISc) for XPS measurement.

Reference

- Lokeswara, G.V.; Reddy, Rama Moorthy, L.; Chengaiah, T.; Jamalaihah, B.C.; *Adv.Mat.Lett.*, **2013**, *4*, 841.
DOI: [10.5185/amlett.2013.3453](https://doi.org/10.5185/amlett.2013.3453)
- Bourenane, K.; Keffous, A.; Nezzal G.; *Vacuum*, **2007**, *81*, 663.
DOI: [10.1016/j.vacuum.2006.09.009](https://doi.org/10.1016/j.vacuum.2006.09.009)
- Phae-ngam, W.; Kosalathip, V.; Kumpeerapun, T.; Limsuwan, P.; Dauscher, A.; *J. Appl. Sci.*, **2011**, *11*, 3625.
DOI: [10.3923/jas.2011.3625.3629](https://doi.org/10.3923/jas.2011.3625.3629)
- Zakery A; and S.R. Elliot; *J. Non-Cryst.Solids*, **2003**,*330*, 1.
DOI: [10.1016/j.jnoncrysol.2003.08.064](https://doi.org/10.1016/j.jnoncrysol.2003.08.064)
- Chou, J. C.; Yang, S. Y.; Wang, Y.S; *Matter. Chem. Phys.***2003**, *78*(3), 666.
DOI: [10.1016/j.jpms.2010.08.022](https://doi.org/10.1016/j.jpms.2010.08.022)
- Peng, C.; Cheng, L.; Mansuripur, L.; *J. Appl. Phys.*, **1997**, *82*,4183
DOI: [10.1063/1.366220](https://doi.org/10.1063/1.366220)
- Girgis, S. Y.; Selim, A.M.; *J. Phy: Condense Matter*, **2007**, *19*, 116213.
DOI: [10.1088/0953-8984/19/11/116213](https://doi.org/10.1088/0953-8984/19/11/116213)
- Nicolas, H.O.;Jacques, M. Lanie.; Real Valee; Alain Villeneuve.; *Opt. Lett.* **2003**,*28*, 965
DOI: [10.1364/OL.28.000965](https://doi.org/10.1364/OL.28.000965)
- Zhang, Z; Gu, Y; Song, S; Cheng, Y; Liu, B, Zhu Y; Zhou, D; Feng, S; *J.Appl.Phys.*, **2014**, *116*, 074304.
DOI: [10.1063/1.4891731](https://doi.org/10.1063/1.4891731)
- Takats, V; Miller, A C; Jain, H; Kovalskiy, A; Kokenyesi, S; *Thin Solid Films*, **2011**, *519*, 3437.
DOI: [10.1016/j.tsf.2011.01.263](https://doi.org/10.1016/j.tsf.2011.01.263)
- Bilanych, V; Komanicky, Feher A; Kuzma, V; Rizak, V; *Thin Solid Films*, **2014**, *571*, 175.
DOI: [10.1016/j.tsf.2014.10.067](https://doi.org/10.1016/j.tsf.2014.10.067)
- Popescue M.A; *Non-Crystalline Chalcogenides*; Kluwer Academic Publ.; 2000, p.293.
ISBN: [10.0792366484](https://doi.org/10.0792366484)
- Zou, L.E.; Chen, B. X.; L. P. Du, H. Hamanaka, and M. Iso; *J. Appl. Phys.***2008**,*103*, 123523 .
DOI: [10.1063/1.2942397](https://doi.org/10.1063/1.2942397)
- Marquez E.; Wagner T.; Gonzalez-Leal J. M.; A.M. Bernal-Olive.; Prieto-Aleon R.;Jimenez-Garay R.; Ewen P.J.S.; *J. Non-Cryst.Solids*, **2000**, *274*, 62.
DOI: [10.1016/S0022-3093\(00\)00184-8](https://doi.org/10.1016/S0022-3093(00)00184-8)
- T. L. Barr and S. Seal; *J. Vac. Sci. Technol. A*,**1995**, *13*, 1239 .
DOI: [10.1116/1.579868](https://doi.org/10.1116/1.579868)
- Swanepoel, R.; *J. Phys. E: Sci. Instrum*, **1983**, *16*, 1214.
DOI: [10.1088/0022-3735/16/12/023](https://doi.org/10.1088/0022-3735/16/12/023)
- Moss, T.; *Optical Properties of Semiconductors*, London: Butterworth **1959**.
ISBN: [10.0444891013](https://doi.org/10.0444891013)
- Tichy, L.; H. Ticha and P. Nagels.; *Mater.Lett.***1998**, *36*, 294.
DOI: [10.1016/S0167-577X\(98\)00048-2](https://doi.org/10.1016/S0167-577X(98)00048-2)
- Naik R.; Parida, S.K.; Kumar, C.;Ganesan, R.; Sangunni, K.S.;*J. Alloys. Comp.*, **2012**, *522*,172.
DOI: [10.1016/j.jallcom.2012.01.144](https://doi.org/10.1016/j.jallcom.2012.01.144)
- Naik, R.; Jena, S.; Ganesan, R.;Sahoo, N.K.; *Phys. Status Solidi B* , **2013**, *251*, 661.
DOI: [10.1002/pssb.201350060](https://doi.org/10.1002/pssb.201350060)
- Stabl, M.; Tichy, L.; *Solid State Sciences*, **2005**, *7*, 201.
DOI: [10.1016/j.solidstatesciences.2004.10.023](https://doi.org/10.1016/j.solidstatesciences.2004.10.023)
- Tauc, J.; *Amorphous and liquid semiconductor*, (New York, Plenum Press). **1974**, 179.
ISBN: [0-306-307774](https://doi.org/0-306-307774)
- Ahamad, S.;Gonaie,M.;Khan,M.S.;Zulfequar,M.; *Adv. Mat. Lett.* **2014**, *5*(9), 511
DOI: [10.5185/amlett.2014.590](https://doi.org/10.5185/amlett.2014.590)
- Mott, N.F.; Davis, E.A.;Electronic process in Non-crystalline materials, Clarendon: Oxford, **1979** pp-382/428
ISBN: [10.0198512880](https://doi.org/10.0198512880)
- Nang, T. T.; Okuda, M.;Matsushita,T.;Yakota, S.;Suzuki, A.; *Jap.J. Appl. Phys.*,**1976**, *15*, 849.
DOI: [10.1143/JJAP.15.849](https://doi.org/10.1143/JJAP.15.849)
- Fritzsche, H.;, *Philos. Mag. B*, **1993**, *68*, 561.
DOI: [10.1080/13642819308217935](https://doi.org/10.1080/13642819308217935)
- Pamukueiva,V.;Szekeres, A.; *J. Opt. Adv. Mater*, **2005**, *7*, 1277.
- Knotek, P.; Tichy, L.; Arsova, D.; Ivanova, Z. G.; Ticha, H.; *Mater. Chem. Phys.*, **2010**, *119*, 315
DOI: [10.1016/j.matchemphys.2009.09.003](https://doi.org/10.1016/j.matchemphys.2009.09.003)
- Adarsh, K. V.; Naik, R.;Sangunni, K.S.;Kokenyesi, S.; Jain, H.;Miller, A. C.; *J. Appl. Phys.* **2008**, *104*, 053501.
DOI: [10.1063/1.2973460](https://doi.org/10.1063/1.2973460)
- Urbach, F.; *Phys. Rev.* **1953**, *92*, 1324.
DOI: [10.1103/PhysRev.92.1324](https://doi.org/10.1103/PhysRev.92.1324)
- Elliot, S.R.; *The Physics and Chemistry of Solids*, John Wiley & Sons: UK, **1998**.
ISBN: [0471981958](https://doi.org/0471981958)
- Cody, G.D.; Tiedje, T.; Abeles, B.; Brooks, B.; Goldstein, Y.; *Phy. Rev. Lett.* **1981**,*47*, 1480.
DOI: [10.1103/PhysRevLett.47.1480](https://doi.org/10.1103/PhysRevLett.47.1480)
- Li, W.; Seal, S.; Lopez, C.; Richardson, K. A.; *J. Appl. Phys.* **2002**, *92*, 7102.
DOI: [10.1063/1.1518134](https://doi.org/10.1063/1.1518134)
- Shpotyuk, O.; Balistika, V.; Filipecki, J.; *J. Phys: Conf. Series*, **2005**, *21*, 81.
DOI: [10.1088/1742-6596/21/1/013](https://doi.org/10.1088/1742-6596/21/1/013)
- Choi, D. Y.; Madden, S.; Rode, A.;Wang, R.; Davies, B. L.; *J. Appl. Phys.* **2007**,*102*, 083532.
DOI: [10.1063/1.2798936](https://doi.org/10.1063/1.2798936)
- Jain, H.; Kovalsky, A.; Miller, A.; *J. Non-Cryst. Solids*, **2006**, *352*, 562
DOI: [10.1016/j.jnoncrysol.2005.11.044](https://doi.org/10.1016/j.jnoncrysol.2005.11.044)

Advanced Materials Letters

Copyright © VBRI Press AB, Sweden
www.vbripress.com

Publish your article in this journal

Advanced Materials Letters is an official international journal of International Association of Advanced Materials (IAAM, www.iaamonline.org) published by VBRI Press AB, Sweden monthly. The journal is intended to provide top-quality peer-review articles in the fascinating field of materials science and technology particularly in the area of structure, synthesis and processing, characterisation, advanced-state properties, and application of materials. All published articles are indexed in various databases and are available download for free. The manuscript management system is completely electronic and has fast and fair peer-review process. The journal includes review article, research article, notes, letter to editor and short communications.

